applied sciences

MDPI

Article

Comparative Analysis of Target Displacements in RC Buildings for 2023 Türkiye Earthquakes

Ercan Işık [1,*], Fatih Avcil [1,*], Aydın Büyüksaraç [2] and Enes Arkan [3]

[1] Department of Civil Engineering, Bitlis Eren University, Bitlis 13100, Türkiye
[2] Çan Vocational School, Çanakkale 18 Mart University, Çanakkale 17400, Türkiye; absarac@comu.edu.tr
[3] Department of Architecture, Bitlis Eren University, Bitlis 13100, Türkiye; earkan@beu.edu.tr
* Correspondence: eisik@beu.edu.tr (E.I.); favcil@beu.edu.tr (F.A.)

Abstract: The Kahramanmaraş (Türkiye) earthquake on 6 February 2023, one of the largest earthquakes of the century, caused the collapse or severe damage of thousands of structures. This catastrophic disaster resulted in over 53,000 fatalities and rendered many structures unusable. This study addresses the observed damage in reinforced concrete (RC) structures, which constituted the majority of the existing urban building stock. In this study, firstly, information about the destructive Kahramanmaraş earthquakes was given. The predicted PGAs in the last two earthquake hazard maps used in Türkiye were compared with the measured PGAs from actual earthquakes to determine whether the earthquake hazard is adequately represented for eleven affected provinces in the earthquake region. The damages in RC structures were evaluated within the scope of civil and earthquake engineering. Structural analyses for the model created to represent mid-rise RC buildings in the region were carried out separately for each province using predicted and measured PGAs. Additionally, target displacements that were used in performance-based earthquake engineering for damage prediction, were examined comparatively for all provinces. While the predicted earthquake hazard and targeted displacements were exceeded in some provinces, there was no exceedance in the other provinces. The realistic representation of earthquake hazards will allow the predicted displacements for various performance levels of structures to be determined in a much more realistic way. Consequently, the performance levels predicted for the structures will be assessed with greater accuracy. The study highlights the importance of accurately presenting earthquake hazards to predict building performance effectively.

Keywords: Kahramanmaraş; earthquake; target displacement; PGA; reinforced-concrete

Academic Editors: Amir M. Yousefi, Bijan Samali and Sang-Hyo Kim

Received: 11 February 2025
Revised: 31 March 2025
Accepted: 3 April 2025
Published: 5 April 2025

Citation: Işık, E.; Avcil, F.; Büyüksaraç, A.; Arkan, E. Comparative Analysis of Target Displacements in RC Buildings for 2023 Türkiye Earthquakes. *Appl. Sci.* **2025**, *15*, 4014. https://doi.org/10.3390/app15074014

1. Introduction

Studies to be conducted after destructive earthquakes provide critical information to both realistically present the situation in the affected region after the earthquake and to reduce the effects of similar disasters in the future. It provides suggestions for improvement and reconstruction processes by correctly assessing the condition of structures that have suffered different levels of damage or destruction. Studies to be conducted in earthquake-affected regions can reveal whether the earthquake hazard is adequately represented or not, and can also reveal the inadequacy of current construction and structural engineering techniques. These studies contribute to the development of earthquake-resistant building design rules. Within the scope of this study, it was tried to reveal whether the earthquake hazard was adequately represented for 11 provinces of Türkiye affected by the 2023 Kahra-

manmaraş earthquakes and the effect of this hazard on structural analyses especially within the scope of performance-based earthquake engineering.

Two significant earthquakes occurred independently of one another, nine hours apart, on 6 February 2023, in the East Anatolian Fault Zone (EAFZ), the main tectonic zone in Türkiye, located in the Alpine-Himalayan earthquake belt. In addition to occurring on the same day, these earthquakes were large, shallow, and affected a vast area. The aftershocks caused even more loss of life and property. Examining and evaluating structural damage after each devastating earthquake provides valuable insight for presenting earthquake hazards more realistically and developing earthquake-resistant building design principles. Each of these studies can be appraised as a case study.

There are many studies examining theoretically and numerically the causes of damage to different structural systems following earthquakes in different settlements around the world. Goda et al. [1] evaluated the damages from the 2015-Gorkha (Nepal) earthquake through field investigations. Milani and Valente [2] investigated the collapse mechanisms using comparative static pushover and limit analyses for seven churches damaged in the 2012 Italy earthquake. Zhang and Jin [3] examined building damage after the Wenchuan earthquake in the context of cause and effect. Clifton et al. [4] investigated the damage to steel buildings following the Christchurch earthquake series. Lagomarsino [5] examined the structural damage in churches after the L'Aquila earthquake. Mimura et al. [6] evaluated the damage caused by the earthquake and tsunami in Japan. Mangalathu et al. [7] classified earthquake damage using artificial intelligence after the 2014 South Napa earthquake. Valente and Milani [8] examined earthquake damage and collapse mechanisms for a castle in Italy after the earthquake. Stepinac et al. [9] classified the damage in settlements after the Zagreb earthquake in their study. Ademović et al. [10] conducted a damage assessment and subsequent strengthening recommendations for a historical masonry structure after the 2020 Zagreb earthquake. Pantò et al. [11] used a macro-modeling approach to assess masonry arch bridges under earthquake loading. Naik et al. [12] evaluated the environmental effects of the Hualien earthquake. Naik et al. [13] examined the damage in Medieval monuments around New Delhi in detail and proposed a new approach. Sugimori [14] examined structural damage specifically for the 1855 Edo earthquake. Qu et al. [15] investigated the seismic failures in buildings after the Luding earthquake. Tena-Colunga [16] explored the relationship between earthquake failures and structural irregularities. Nemutlu et al. [17], Işık et al. [18], and Caglar et al. [19] investigated the failures in different types of structures after the Sivrice (Elazığ) earthquake.

There are many studies that have evaluated the earthquake damages in different structural systems following 6 February 2023, Kahramanmaraş earthquakes within the scope of structural and earthquake engineering. Each of these studies, conducted for these earthquakes considered the disaster of the century for Türkiye, will contribute to the development of both seismic design code and earthquake hazard map. Işık [20] examined the seismic damage in adobe structures following earthquakes while Avcil [21] focused on the damage to the prefabricated structures. İnce [22], Ivanov and Chow [23], and Işık et al. [24] studied the failures in RC buildings in Adıyaman province. Yuzbasi [25] studied the impact of the 6 February 2023, disasters in Türkiye. Bol et al. [26] and Cetin et al. [27] investigated soil liquefaction following the 2023 Kahramanmaraş disasters. Arslan [28] examined the impacts of earthquakes on existing prefabricated structures in the context of codes. Avğın et al. [29] studied the impacts of earthquakes on different structural systems in Kahramanmaraş province. Binici et al. [30] examined the earthquake performances of buildings after the earthquake and provided insights into the lessons to be learned. Demir et al. [31] investigated the causes of the significant destruction of structures in earthquakes. Ozturk [32] studied the impacts of earthquakes on RC buildings and made

recommendations for the development of design guidelines. Nemutlu et al. [33] compared the actual economic losses and loss of life after earthquakes with the estimated results. Balun [34] compared seismic parameters specifically for the earthquake region. Sivrikaya et al. [35] examined in detail the effect of local soil conditions on seismic fragility for 400 different RC buildings that collapsed during these earthquakes. Altunışık et al. [36] comprehensively evaluated the damage to RC structures based on observations. Şen et al. [37] investigated the seismic behavior of a hospital building with base isolation located in an earthquake region. Erbaş et al. [38] studied the damage modes in RC structures and provided reinforcement recommendations for such structures. Akar et al. [39] and Flora et al. [40] examined the damages in Gölbaşı district of Adıyaman province from both geotechnical and structural perspectives. Tapia-Hernández et al. [41,42] evaluated the damage in steel structures and hospital-type structures in the earthquake area. Tan [43] investigated the effect of infill walls on a heavily damaged RC building model. Işık et al. [44] compared the target displacement values for twenty different settlements on the EAFZ where the earthquakes occurred. In addition to these studies, there are others in which damages in RC structures are examined based on observation, damage classifications using different structural assessment methods, and structural weaknesses/irregularities are examined through numerical models [45–54]. In most of these studies, the damage was evaluated based on observation, and recommendations were made. General structural failures in RC structures during these earthquakes are discussed within the scope of this paper. Target displacement values for an RC building model selected as an example for eleven provinces primarily affected by earthquakes were obtained separately for both earthquakes and the proposed earthquake hazard.

Large-scale structural damage caused by earthquakes and the resulting fatalities have made performance-based design and assessment of structures essential [55,56]. One of the aims of earthquake-resistant building design is to ensure that buildings can resist a potential earthquake without suffering excessive damage. The seismic performances of structures under the influence of an earthquake can be determined through structural analyses. Building performance analysis is one of the most crucial stages in earthquake-resistant building design and strengthening. In performance-based earthquake engineering, it is essential to determine target displacements for damage prediction when specific performance thresholds of building elements are achieved. Once the displacement demand in a building is met during a seismic event, it could be assessed if the anticipated performance target for the building has been reached [57,58]. Damage grades that could take place in structural system members under design ground motion can be quantitatively determined using the performance-based design and assessment technique. This method can verify whether the failure is still within allowable limits for each relevant member. Acceptable failure limits have been determined in a way that aligns with the performance targets intended for various earthquake stages [59–61]. The key objective of performance-based modeling is to identify the structural requirements of the building subject to soil motion. A precise characterization of ground motion properties and their correlation is required for the proper calculation of structural demands [62–64]. The maximum horizontal ground acceleration, or peak ground acceleration (PGA), is the single most often used determinant in earthquake hazard calculations. The fact that the design spectra suggested in earthquake specifications may be scaled using PGA or factors related to PGA is one of the most significant justifications for utilizing the PGA. Furthermore, numerous studies in the literature address target displacements in buildings for different topics. Işık [65] studied the displacements of earthquake epicenters during the instrumental period in Türkiye. Maidi and Shufrin [66] explored a different method for evaluating the earthquake resistance of existing buildings and determining the need for seismic retrofitting through external reinforcement. Bilgin

et al. [67] obtained target displacements by considering the minimum structural cases for various countries. Ricci et al. [68] performed incremental dynamic studies on 48 infilled RC buildings with varying design peak ground accelerations (PGAs), story numbers, and infill typologies. Khan [69] investigated the impact of the entrance ground motion on the performance point by obtaining the seismic performance points of a 5-story RC frame structure located in Zone-IV, symmetrical in plan, exposed to three different PGA levels as the entrance ground motion.

In this study, firstly, the impacts of the 6 February, major Kahramanmaraş earthquakes on RC structures were evaluated based on site observation. For this purpose, information about the Kahramanmaraş earthquakes is provided. PGAs and PGVs were attained for different exceedance probabilities from the current earthquake hazard map for Hatay, Kahramanmaraş, Adıyaman, Malatya, Kilis, Gaziantep, Elazığ, Şanlıurfa, Osmaniye and Diyarbakır, which are the 11 provinces primarily affected by these earthquakes. The seismic parameters for these provinces were compared based on the most recent earthquake hazard maps and seismic design codes in Türkiye. An attempt was made to reveal the level at which the seismic hazard in these provinces has changed. In the next stage of the study, the damage in RC structures, which formed the dominant building stock in the earthquake region, was examined in detail based on observation within the scope of earthquake and civil engineering. Numerical analyses were performed on the structural model created to represent mid-rise RC structures in the earthquake region. In this structural model, which does not contain any irregularities, other structural characteristics remained unchanged. Target displacements were obtained for all provinces based on predicted PGAs in the last two earthquake hazard maps and for the highest measured PGAs during the earthquakes. Target displacements were obtained separately for eleven different provinces in the earthquake region. The main goal of this paper is to compare the measured and predicted PGA for the Kahramanmaraş earthquakes and to determine whether the earthquake hazard and structural demands are adequately represented. There is no comparative study currently in the literature for the provinces most affected by these earthquakes. In this manner, it will be clearly shown whether the earthquake hazard is properly represented for these provinces using the last two earthquake hazard maps in the country. At the same time, an attempt was made to accurately determine the magnitude of the earthquakes. Another key objective of the study is to examine the effect of predicted and measured PGAs on target displacement values.

Target displacements are a fundamental factor determining the earthquake reliability and resistance of structures in earthquake performance analyses used to determine the effects of seismic events on structures. Whether or not structures provide their predicted earthquake performance depends on the accurate calculation of displacement limits. Therefore, target displacement analyses in earthquake engineering are essential for assessing structural performance. Target displacements, which are used to determine the level of damage to structures, are essential in assessing the seismic performance of structures. Earthquake performance analysis usually requires a displacement-based assessment. Most earthquake codes require structures to keep target displacements within certain limits. In this approach, the displacements of structures are directly considered as safety and performance criteria. Exceeding these limits indicates that the expected performance levels of the structure will not be achieved. Therefore, it is necessary to accurately determine the displacement targets of structures to ensure the correct seismic performance. In this context, this study reveals whether the target displacements are sufficient for eleven different provinces in the earthquake region.

The key factor that sets this study apart from others is that it is the first detailed study conducted on eleven different provinces in the earthquake region. It is believed that this

comprehensive study, which covers both earthquake hazards and target displacements, will serve as a valuable resource for the development of seismic design codes and earthquake hazard maps. By presenting the earthquake hazard in a realistic and sufficient manner, the target displacements used to assess the seismic performance of structures will be determined with much greater accuracy. As a result, this study will be one of the first studies to comparatively examine earthquake hazard and structural analyses for the entire region affected by the 2023 Kahramanmaraş earthquakes. It will reveal the need to update seismic hazard analyses, especially for settlements where earthquake hazard is not adequately represented. At the same time, recommendations were made considering the causes of damage in RC structures.

2. Tectonic Structure of Türkiye and 2023 Kahramanmaraş Earthquakes

Türkiye's geographic location, along with the interaction of the Eurasian-African and Eurasian-Arabian plates, makes it susceptible to frequent earthquakes. Examining the tectonic system in which Türkiye is situated, it is evident that Eastern Anatolia is compressed by the Arabian Plate as it moves northward toward the Eurasian Plate. The North Anatolian Fault Zone (NAFZ) and the East Anatolian Fault Zone (EAFZ), which developed due to the resistance of the Eurasian Plate in the north, exert pressure on the Anatolian Plate. This results in the Anatolian Plate moving westward (Figure 1). The EAFZ, which is approximately 580 km in length, is one of the seismically active regions in Türkiye and has experienced numerous significant earthquakes. The southeastern boundary of the Anatolian Plate is formed by the left-lateral strike-slip EAFZ, which intersects the North Anatolian Fault Zone (NAFZ) in Karlıova. Similarly, the DSFZ and EAFZ converge near Antakya. The simplified tectonic map of Türkiye is given in Figure 1.

On the contrary, it stretches southwestward in seven distinct sections from Karlıova to the Gulf of İskenderun [70,71]. These strike-slip faults are the site of large, catastrophic earthquakes [72]. This area has experienced catastrophic earthquakes for about 2000 years, according to historical and instrumental records [73–76]. Historical earthquakes originate at the northeastern edge of the EAFZ and move southwestward. The central and southwestern regions of the EAFZ have the highest concentration of historical earthquakes. Over the past 500 years, no earthquake strong enough to create a surface rupture has occurred in the Gölbaşı-Türkoğlu stretch, where the fault bends toward the southwest.

The M_w = 7.7 and 7.6 magnitude earthquakes that struck Kahramanmaraş on Monday, 6 February 2023, just nine hours apart, marked the beginning of a series of major earthquakes in a short period, including additional quakes with magnitudes of 6.6, 5.7, 6.0, and 6.4. Over 53,000 people were killed and more than 100,000 were injured in eleven provinces as a result of these earthquakes, leaving over 500,000 homes uninhabitable. The likelihood of distinct primary shocks is increased when considering the fault systems involved in these disasters and the fact that nearly all of the earthquakes occurred along separate fault segments. As the EAFZ runs through this region, the earthquakes are also seen as stemming from a single tectonic movement. Because of the region's intricate tectonic structure, earthquakes have evolved into interconnected phenomena. As a result, Türkiye, with its dense and complex tectonic members, has experienced many earthquakes to date and will likely continue to do so. The values measured for both earthquakes by various sources are shown in Table 1.

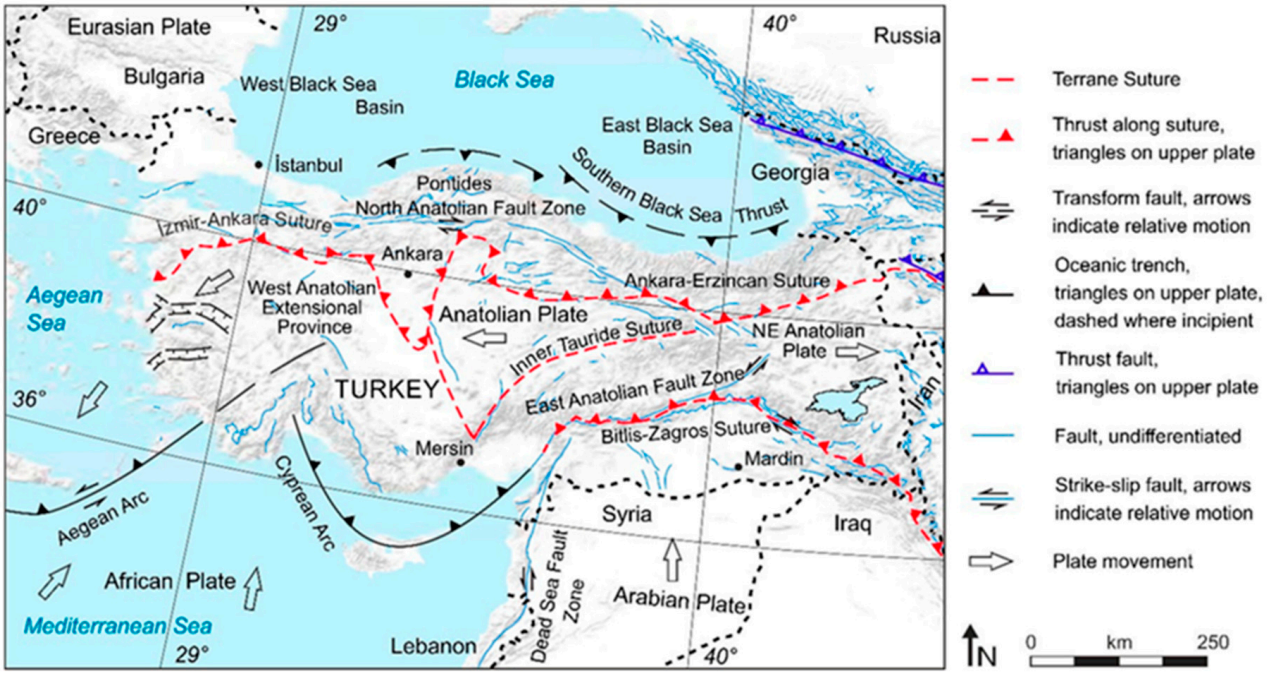

Figure 1. Simplified tectonic map of Türkiye and surroundings [77].

Table 1. Details from two varied sources regarding the earthquakes that happened in Türkiye.

Date/Time	Coordinates (N-E)	Locations	Magnitudes (Mw)	Depths (km)	Sources	Equal Intensities
6 February 2023 04:17:34 (TSI)	37.288° and 37.043°	Pazarcık	7.8	10.0	USGS	XI (11.2)
	37.225° and 37.021°		7.7	8.60	AFAD	XI (11.28)
6 February 2023 13:24:47 (TSI)	38.089° and 37.239°	Elbistan	7.5	10	USGS	X-XI (10.75)
	38.024° and 37.203°		7.6	7.0	AFAD	XI (11.44)

The highest measured PGAs for the 2023 Kahramanmaraş earthquakes, which were the worst disaster of the century for Türkiye, are illustrated in Table 2. The earthquakes caused very high accelerations in some provinces of the region. In particular, provinces such as Kahramanmaraş, Hatay, Adıyaman, and Gaziantep experienced significantly high accelerations. These accelerations resulted in destructive effects on most structures. Soil properties have been one of the factors directly affecting the magnitude of acceleration values. Accelerations were especially pronounced on soft soils, leading to soil liquefaction and increased damage in settlements. It was observed that structures before 2000 in particular have suffered more damage.

The eleven provinces most affected by the Kahramanmaraş earthquakes are illustrated on the map in Figure 2.

The highest PGAs measured in eleven cities significantly affected by the earthquake are illustrated in Table 3.

Table 2. The highest peak ground accelerations for the 2023 Kahramanmaraş earthquakes [78].

Station Code	Latitude	Longitude	Province	District	PGA-NS (cm/s^2)	PGA-EW (cm/s^2)	PGA-UD (cm/s^2)	R_{epi} (km)	Distance to Fault Zone (km)
6 February 2023 04:17 M_w = 7.7 Pazarcık/Kahramanmaraş Depth = 8.6 km									
4614	37.4851	37.2977	Kahramanmaraş	Pazarcık	2016.99	2039.20	1582.62	31.42	8.1
3129	36.1911	36.1343	Hatay	Defne	1351.50	1198.74	716.94	146.39	6.6
3126	36.2202	36.1375	Hatay	Antakya	1178.12	999.38	921.57	143.54	4.8
3141	36.3726	36.2197	Hatay	Antakya	961.12	868.82	722.66	125.42	0.8
3125	36.2380	36.1326	Hatay	Antakya	822.62	1121.95	1151.56	142.15	3.1
6 February 2023 13:24 M_w = 7.6 Elbistan/Kahramanmaraş Depth = 7 km									
4612	38.0239	36.4818	Kahramanmaraş	Göksun	635.45	523.21	494.91	66.68	5.8
4406	38.3438	37.9737	Malatya	Akçadağ	467.20	409.31	318.75	70.17	0.45
0131	37.8566	36.1153	Adana	Saimbeyli	402.32	331.69	85.29	101.83	28.8
4631	37.9663	37.4276	Kahramanmaraş	Nurhak	337.38	388.61	610.04	21.43	0.45
4409	38.5606	37.4907	Malatya	Darende	287.04	218.04	124.28	56.86	48.0

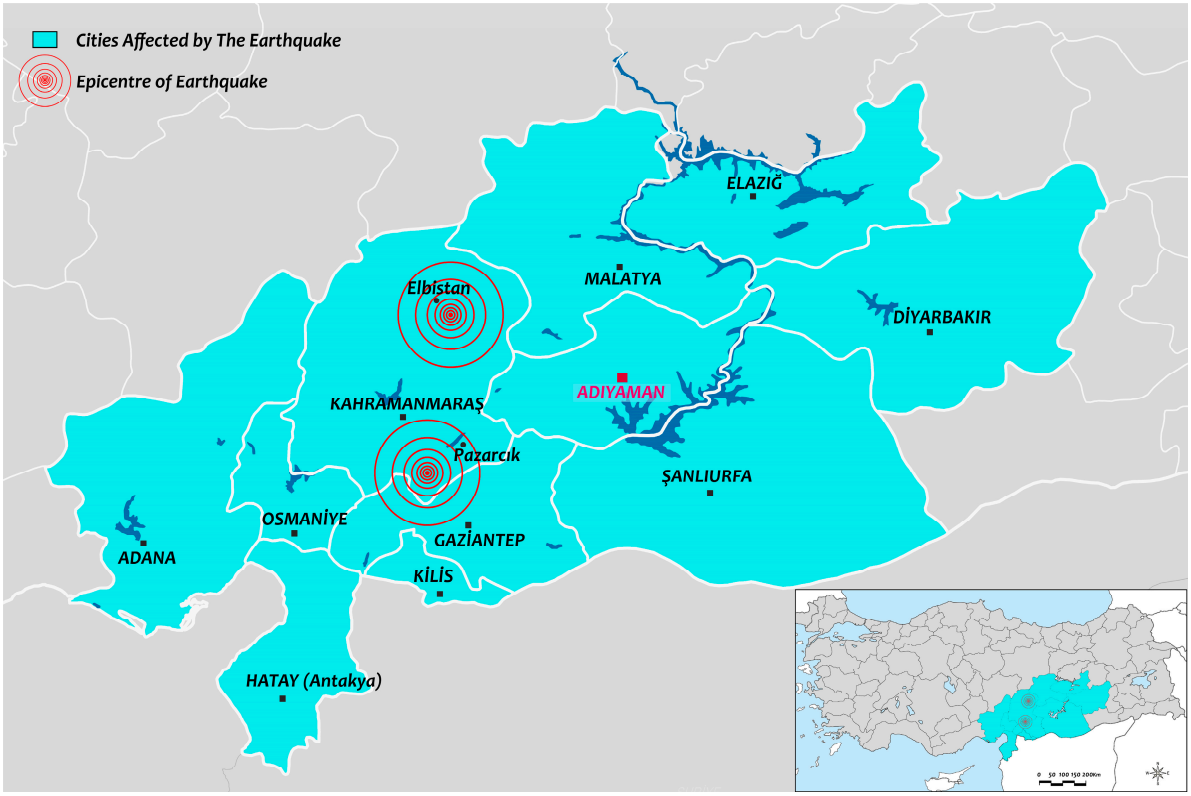

Figure 2. The epicenter of the 2023 Kahramanmaraş earthquakes and earthquake region.

Table 3. The highest measured PGAs in eleven provinces [78].

Pazarcık M_w = 7.7				Elbistan M_w = 7.6			
Station	Province/District	PGA (cm/s^2)	R_{epi} (km)	Station	Province/District	PGA (cm/s^2)	R_{epi} (km)
4614	K.Maraş/Pazarcık	2039.20	31.42	4612	K.Maraş/Göksun	635.45	66.68
3135	Hatay/Arsuz	1372.07	142.15	4406	Malatya/Akçadağ	467.20	70.17
0201	Adıyaman/Centre	879.95	120.12	0131	Adana/Saimbeyli	402.30	101.83
2718	Gaziantep/Islahiye	654.43	48.30	0213	Adıyaman/Tut	126.62	68.73
8002	Osmaniye/Bahçe	336.56	43.91	2703	Gaziantep/Şahinbey	93.68	115.06
6304	Şanlıurfa/Bozova	238.23	130.27	3138	Hatay/Hassa	78.11	162.37
4414	Malatya/Kale	163.84	195.07	2308	Elazığ/Sivrice	69.80	185.23
0131	Adana/Saimbeyli	159.77	103.35	8003	Osmaniye/Centre	66.60	140.65
2104	Diyarbakır/Ergani	116.47	262.22	7901	Kilis/Centre	50.91	153.88
2310	Elazığ/Baskil	60.46	211.70	2107	Diyarbakır/Çermik	47.61	196.48
7901	Kilis/Centre	53.11	64.70	6306	Şanlıurfa/Akçakale	36.00	213.70

As a result of the earthquakes it has experienced, Türkiye has made significant changes in both earthquake hazard maps and earthquake regulations over time.

The spectral accelerations recorded during the Pazarcık and Elbistan earthquakes at different ground motion stations in the E-W and N-S directions are shown in Figures 3 and 4 respectively.

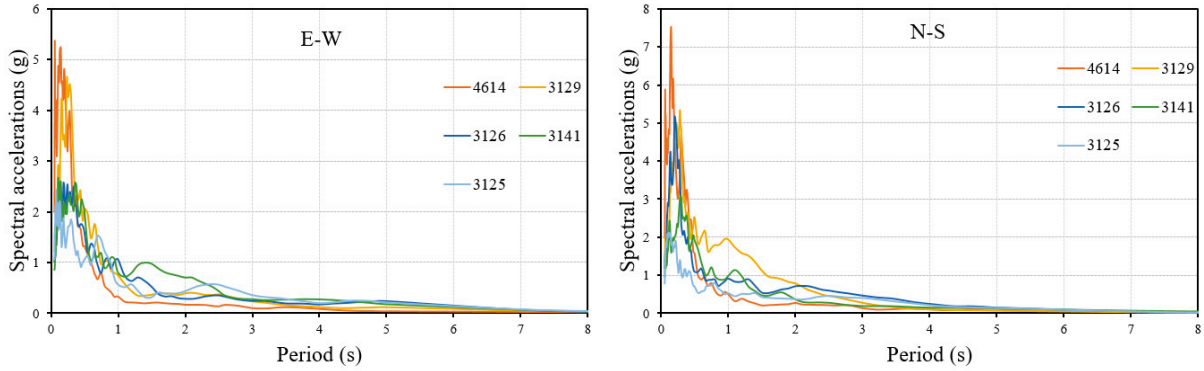

Figure 3. Spectral accelerations measured during Pazarcık (M_w = 7.7) earthquake.

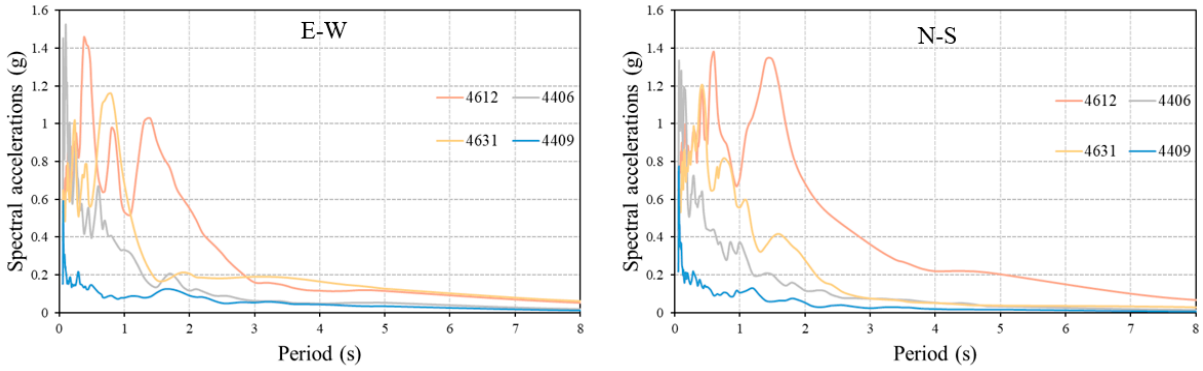

Figure 4. Spectral accelerations measured during the Elbistan (M_w = 7.6) earthquake.

Earthquake Zones map, in use since 1996, was replaced by the Türkiye Earthquake Hazard Map, which was updated in 2019. The earthquake regulation, which has been in use since 2007, was replaced by the Turkish Building Earthquake Regulation in 2019. In this study, seismic parameters for eleven different provinces where the 6 February 2023 earthquakes were most strongly felt, were compared using the last two earthquake hazard maps. In the previous map, seismic parameters were obtained on a regional basis. With the current map, seismic parameters can be obtained separately for different exceedance probabilities for each geographical location and soil class, with the help of the Turkish Earthquake Hazard Map Interactive Web Earthquake Application (TEHMIWA). This application was developed within the scope of the Seismic Hazard Map Update project, which is required in the National Earthquake Strategy and Action Plan for the basic research to be done to reduce the earthquake hazard in the country. In the project, PGA, PGV, and other seismic parameters within the land borders of Türkiye were obtained for different annual exceedance probabilities using the probabilistic seismic hazard methods. The seismic source, earthquake, and ground motion databases formed in Türkiye in recent years were evaluated in the best way in the project, and the country's earthquake hazard map was updated. In the project, seismic sources within the land borders of Türkiye were determined, instrumental and historical earthquake catalogs were compiled, and then seismic parameters were obtained for different exceedance probabilities and ground classes for each geographical location using probabilistic seismic hazard analyses using

earthquake recurrence models and ground motion estimation equations. With the help of this application created as a result of the project, seismic parameters can be obtained for any location. In this study, current seismic parameters were obtained with the help of this application [79]. This work considers four different earthquake ground motion levels, including 2%, 10%, 50%, and 68%, which are included in the current earthquake regulation and have a probability of being exceeded in 50 years. The characteristics of these ground motion levels are shown in Table 4.

Table 4. Levels of the earthquake ground motion [80].

Earthquake Ground Motion Level	Probability of Exceedance (50 Years)	Repetition Period (Year)	Definition
DD-1	0.02	2475	Largest earthquake ground motion
DD-2	0.1	475	Standard design earthquake ground motion
DD-3	0.5	72	Frequent earthquake ground motion
DD-4	0.68	43	Service earthquake ground motion

To make comparisons in this study, an earthquake with a 10% probability of exceedance, the standard earthquake ground motion level in 50 years, which is included in both regulations, was taken into consideration. ZC soil class, which represents moderate soil class, was taken into account. PGAs and PGVs attained for various exceedance of probabilities at random locations from the provincial centers of the eleven provinces most affected by both earthquakes are illustrated in Table 5.

Table 5. Predicted PGAs and PGVs of provinces in the earthquake zone for the current earthquake hazard map.

No.	Province	PGA (g)				PGV (cm/s)			
		2%	10%	50%	68%	2%	10%	50%	68%
1	Hatay	0.890	0.446	0.148	0.100	55.845	27.623	8.336	5.593
2	Kahramanmaraş	0.699	0.380	0.142	0.097	45.258	23.626	8.266	5.598
3	Adıyaman	0.419	0.241	0.098	0.065	29.053	16.118	6.184	4.036
4	Kilis	0.421	0.207	0.079	0.057	27.888	13.683	5.338	3.903
5	Diyarbakır	0.254	0.142	0.061	0.044	17.956	10.493	4.570	3.295
6	Şanlıurfa	0.221	0.110	0.042	0.029	14.355	7.922	3.240	2.279
7	Malatya	0.648	0.344	0.134	0.090	40.782	21.228	7.992	5.326
8	Osmaniye	0.605	0.311	0.114	0.078	37.273	18.248	6.496	4.510
9	Adana	0.450	0.232	0.084	0.057	24.230	11.927	4.578	3.298
10	Elazığ	0.740	0.400	0.155	0.104	48.139	25.074	9.284	6.025
11	Gaziantep	0.320	0.164	0.067	0.049	22.519	11.896	4.894	3.569

The highest PGA value with a 2% probability of exceeding was obtained as 0.890 g for Hatay. The lowest PGA value for this probability of exceedance was 0.221 g for Şanlıurfa. For the eleven provinces considered, the PGA range for a 10% probability of exceedance ranges from 0.110 to 0.446 g. For the same earthquake ground motion level, PGV values ranged from 7.922 to 27.623 cm/s. Table 6 presents a comparison of the PGA values anticipated in the previous seismic zones map with those derived from the current earthquake

hazard map. The design spectrum acceleration coefficient (S_{DS}) forecasted in the previous two earthquake hazard maps that were used in Türkiye is also contrasted in this table.

Table 6. The comparison of the predicted PGA and S_{DS} on the last two maps and codes for the 2023 Kahramanmaraş earthquake region.

No.	Province	Earthquake Zone	1996 PGA (g)	2018 PGA (g)	2018/1996	$S_{DS\ 2007}$	$S_{DS\ 2018}$	$S_{DS\ 2018}/S_{DS\ 2007}$
1	Hatay	1	0.400	0.446	1.115	1.000	1.260	1.260
2	Kahramanmaraş	1	0.400	0.380	0.950	1.000	1.091	1.091
3	Adıyaman	2	0.300	0.241	0.803	0.750	0.728	0.971
4	Kilis	4	0.100	0.207	2.070	0.250	0.631	2.524
5	Diyarbakır	2	0.300	0.142	0.473	0.750	0.413	0.551
6	Şanlıurfa	3	0.200	0.110	0.550	0.500	0.317	0.634
7	Malatya	1	0.400	0.344	0.860	1.000	0.985	0.985
8	Osmaniye	1	0.400	0.311	0.778	1.000	0.877	0.877
9	Adana	2	0.300	0.232	0.773	0.750	0.683	0.911
10	Elazığ	2	0.300	0.400	1.333	0.750	1.147	1.529
11	Gaziantep	3	0.200	0.164	0.820	0.500	0.500	1.000

The PGA value increased with the current earthquake hazard map for the geographical locations considered in the Hatay, Kilis, and Elazığ provinces. In other provinces, the values predicted on the current map have decreased compared to the previous earthquake zone map. While the largest increase was obtained for Kilis province, the largest decrease was obtained for Gaziantep province. Design spectral acceleration coefficients also varied for the geographical locations considered in all provinces except Gaziantep. While they increased in Hatay, Kahramanmaraş, Kilis, and Elazığ provinces, there was a decrease in other provinces. No change was observed in the location selected for Gaziantep province.

A comparative study was conducted to determine whether the earthquake hazard for the 11 provinces affected by the 6 February Kahramanmaraş earthquake was adequately represented on the earthquake hazard maps. For this purpose, the comparison of the PGAs measured in both earthquakes for these provinces, along with the predicted PGAs from the last two earthquake hazard maps used in Türkiye is given in Table 7.

Table 7. Comparison of the measured and predicted PGAs.

No.	Province	Measured Maximum PGA (g)	TSDC-2007 PGA (g) DD-2	Provide or Not	TBEC-2018 PGA (g) DD-2	Provide or Not	TBEC-2018 PGA (g) DD-1	Provide or Not
1	Hatay	1.399	0.400	X	0.446	X	0.890	X
2	Kahramanmaraş	2.079	0.400	X	0.380	X	0.699	X
3	Adıyaman	0.897	0.300	X	0.241	X	0.419	X
4	Kilis	0.054	0.100	√	0.207	√	0.421	√
5	Diyarbakır	0.119	0.300	√	0.142	√	0.254	√
6	Şanlıurfa	0.243	0.200	X	0.110	X	0.221	X
7	Malatya	0.476	0.400	X	0.344	X	0.648	√
8	Osmaniye	0.343	0.400	√	0.311	X	0.605	√
9	Adana	0.410	0.300	X	0.232	X	0.450	√
10	Elazığ	0.071	0.300	√	0.400	√	0.740	√
11	Gaziantep	0.667	0.200	X	0.164	X	0.320	X

While the previous earthquake hazard map used in Türkiye took into account four different earthquake zones, the current map takes each geographical location into account separately. For 2007, the values were determined according to the earthquake zones of the

provinces. For the 1st-degree earthquake zone, it was taken as 0.400 g, for the 2nd-degree earthquake zone, it was taken as 0.300 g, for the 3rd-degree earthquake zone, it was taken as 0.200 g and for the 4th-degree earthquake zone, it was taken as 0.100 g in the previous earthquake zone map in Türkiye. The 2018-PGA values used in this table are obtained directly from TEHMIWA. While the predicted PGAs in the previous earthquake zone map were adequately represented for Kilis, Diyarbakır, Osmaniye, and Elazığ, the measured PGAs for other provinces exceeded the predicted values. In the current earthquake hazard map, the PGAs foreseen for standard design ground motion (DD-2) are sufficient for Kilis, Diyarbakır, and Elazığ, but there is an exceedance for other provinces. On the other hand, the measured PGAs for the largest earthquake ground motion level (DD-1) in Hatay, Kahramanmaraş, Adıyaman, Şanlıurfa, and Gaziantep provinces exceeded the predicted values. These results also clearly reveal the magnitude and destructive effects of these earthquakes in the region. This highlights the magnitude of the earthquakes and the need to update the earthquake hazard maps in the region in light of these two major earthquakes. Taking into account these two major earthquakes and their aftershocks in this region, updating the seismic hazard analyses, especially for these provinces, will enable the earthquake hazard to be presented in a realistic sense. Additionally, it is crucial to take the necessary precautions for the existing building stock and the buildings to be rebuilt in this region.

3. Damage Noted in RC Structures

In the eleven provincial centers most affected by the Kahramanmaraş earthquakes, significant and varied structural damage occurred in different structural systems. While the dominant building stock in rural areas is masonry structures, the dominant building stock in urban areas is RC structures. In this section, the damage examples commonly observed in RC structures of the urban dominant building stock are examined in terms of civil and earthquake engineering. In particular, the damage examples in RC structures from the three provinces affected by the earthquake, Hatay, Kahramanmaraş, and Adıyaman, are taken into consideration. The causes of the damages and their schematic representations are made for better understanding. In this way, the main causes of the damages can be better revealed. Irregularities and weaknesses in RC structures played an active role in the damages. The magnitude of the earthquakes that occurred on the same day and the local ground conditions also directly affected the level of damage. As a result of earthquakes, there was great destruction in RC structures. Examples of RC structures that reached a total collapse mechanism are shown in Figure 5.

Figure 5. Examples of totally collapsed RC structures.

Insufficient interlocking between load-bearing elements in RC structures, strong beam-weak column formations, and weak material properties prevented the RC frame from functioning as a whole. For these reasons, the floors in the building collapsed on top of each other. Such collapses are the ones that make after-earthquake search and rescue efforts most difficult.

In order to understand the destructive impact of earthquakes, a comparison of the building conditions of four sample RC buildings before and after the earthquake is illustrated in Figure 6. The difference in strength and stiffness between stories caused partial or total collapse of the intermediate or ground floors. In such demolitions, it is not possible to strengthen and reuse the structure.

Figure 6. Comparison of some RC building examples before and after the earthquake.

Soil liquefaction is the temporary liquefaction of the soil due to the increase in water pressure between the soil particles as a result of strong vibrations such as earthquakes. This situation can cause damage at different levels by causing the bearing capacity of the soil structure to decrease significantly [81–83]. Examples of such damage are shown in Figure 7.

Figure 7. Soil liquefaction samples in the earthquake region.

This study provides information on the damages commonly encountered in RC structures and their causes based on field observations. In particular, the lack of, or complete failure to apply, earthquake-resistant structural design principles has increased the extent of damage in RC structures. Examples of structural damage in RC buildings, their causes,

and their schematic representations, which are commonly encountered in the earthquake region, are given in Figure 8.

Figure 8. *Cont.*

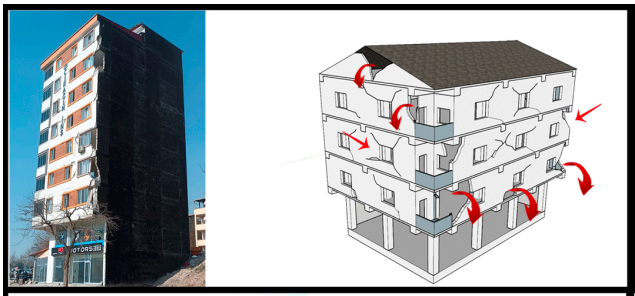	Heavy overhang: Heavy overhangs are one of the factors that cause vertical structural irregularities. These overhangs, added to expand the upper floor's usage area, exhibited negative performance during the earthquake, leading to various levels of damage in many buildings.
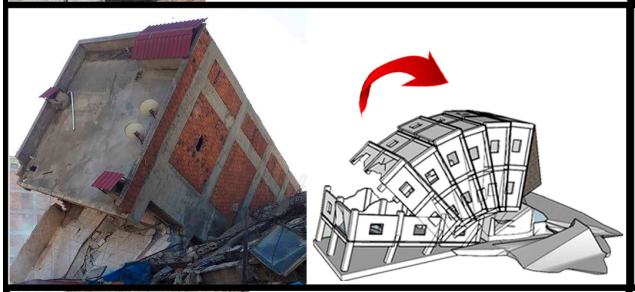	Lateral collapse: Although the frame system of the building remains intact, many buildings collapsed laterally due to ground and foundation failures.
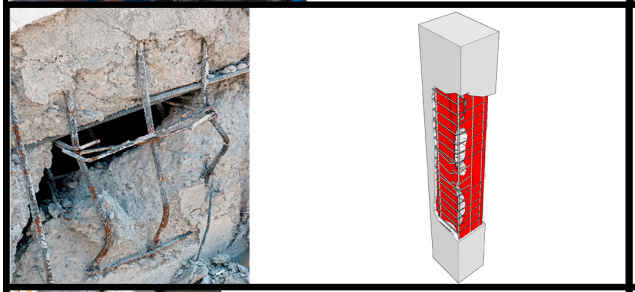	90° hooks instead of 135°: The ends of the stirrups and crossties must be fully hooked (135° bent). In the structure, the type of damage caused by the yielding in the vertical reinforcement, the excessive spacing of the stirrups, and the ends of the stirrups being open outside without bending 135° towards the inside of the column are observed.
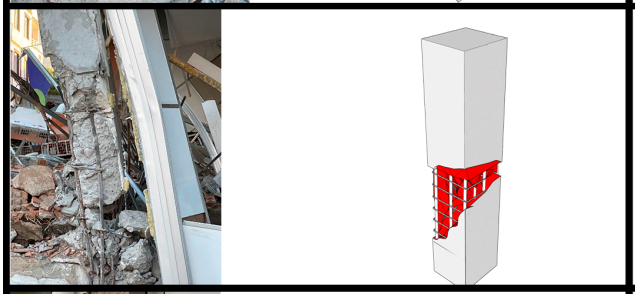	Usage of plain reinforcement: Plain rebar used in many older buildings has been found to cause significant structural damage due to its poor adhesion to concrete. Following the 1998 regulation in Türkiye, the use of ribbed reinforcement became mandatory.
	Inadequate concrete cover: The concrete cover, which increases the durability of reinforced concrete by protecting the reinforcement steel from corrosion, is left at 2.5 cm in normal cases, 4 cm in external members, and more in water structures. Due to the insufficient concrete cover thickness, the concrete coating breaks and falls, causing structural damage to the column.
	Low-strength concrete: Due to the shear effect of the earthquake, cracking and disintegration occurred at lower load levels. Under this load, the column reinforcement separated from the fractured concrete, leading to structural damage.

Figure 8. *Cont.*

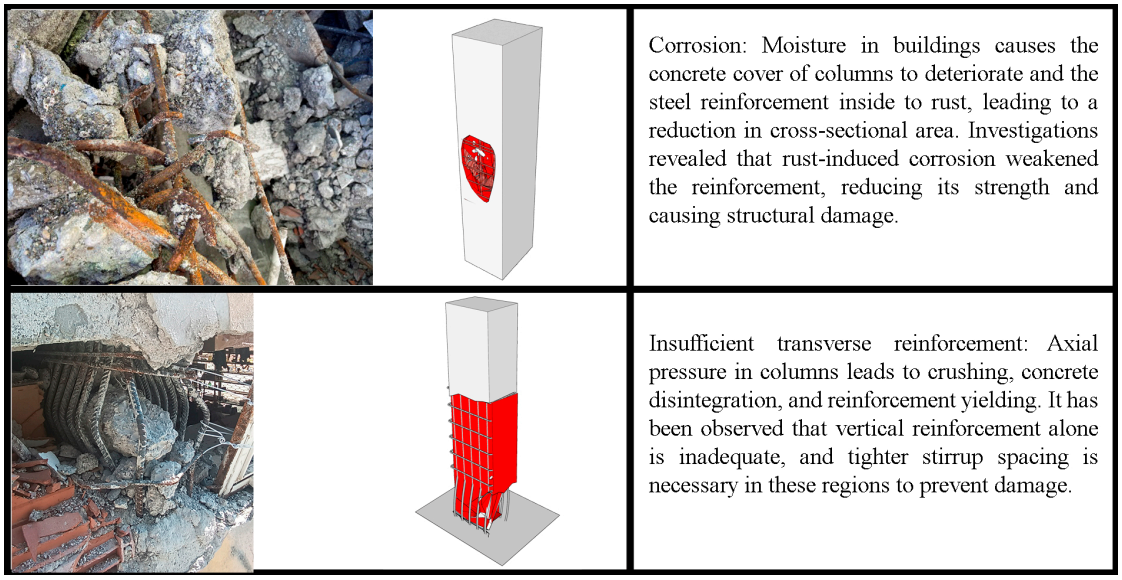

Figure 8. Examples of structural damage commonly observed in RC structures and their schematic representations.

4. Comparison of Target Displacements

The risk posed by earthquakes to human activities and the potential for significant loss of life due to structural damage provide compelling reasons to consider earthquakes in structural design. The earthquake-resistant design aims to create structures that can withstand a certain level of seismic activity without experiencing severe damage. In this context, target displacement limits are established for various performance levels of structures. Structural analyses were conducted to assess whether the Kahramanmaraş earthquakes appropriately reflected the target displacement limit values in the affected buildings.

The dominant building stock in the city centers in the earthquake region consists of RC structures, particularly mid-rise RC structures, which are widely used in the region. The majority of RC structures that suffered varying levels of damage or destruction were mid-rise RC structures. The majority of medium-rise reinforced concrete buildings in the earthquake zone consist of 4–8 stories. In order to represent these structures, a 5-story building without any irregularities was modeled. Material properties in accordance with current seismic design codes were used as design criteria. The structural model was chosen to be symmetrical in both directions. In selecting the model building features, structural characteristics commonly used in practice were taken into account. Structural analyses were carried out for an example RC structure, considering the highest PGA values measured in eleven different provinces in the earthquake region, both from earthquake pairs and the PGAs estimated for these provinces in the last two earthquake hazard maps used in Türkiye. The analyses were performed using Seismostruct-2024 software [84]. In structural analyses, pushover analyses were conducted separately for each province. The RC building model is a 5-story structure with equal floor heights of 3 m. The building has the same span length in the X and Y directions, is symmetrical and each span is chosen as 4.50 m. The 2D and 3D models created for the sample RC structure and the applied loads are shown in Figure 9. RC columns were taken into account as square cross-sections in order not to create weak and strong directions for the structural model. Therefore, structural analyses were performed only in the X direction for all structural models. The RC building model selected as an example was chosen to represent mid-rise RC buildings in the earthquake region.

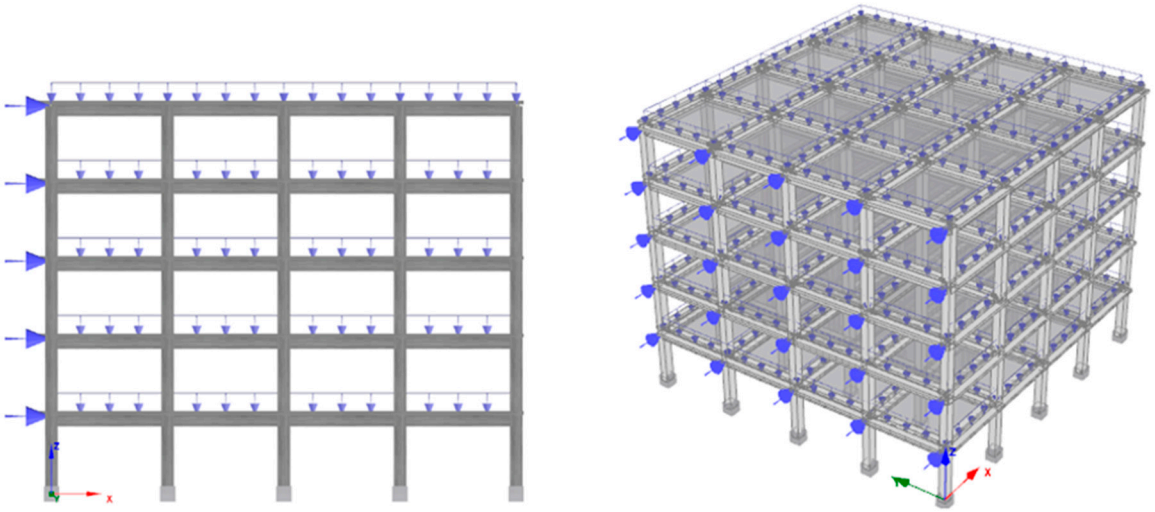

Figure 9. 2D and 3D numerical models of the sample RC structure.

The blueprint of the selected RC structural model is shown in Figure 10.

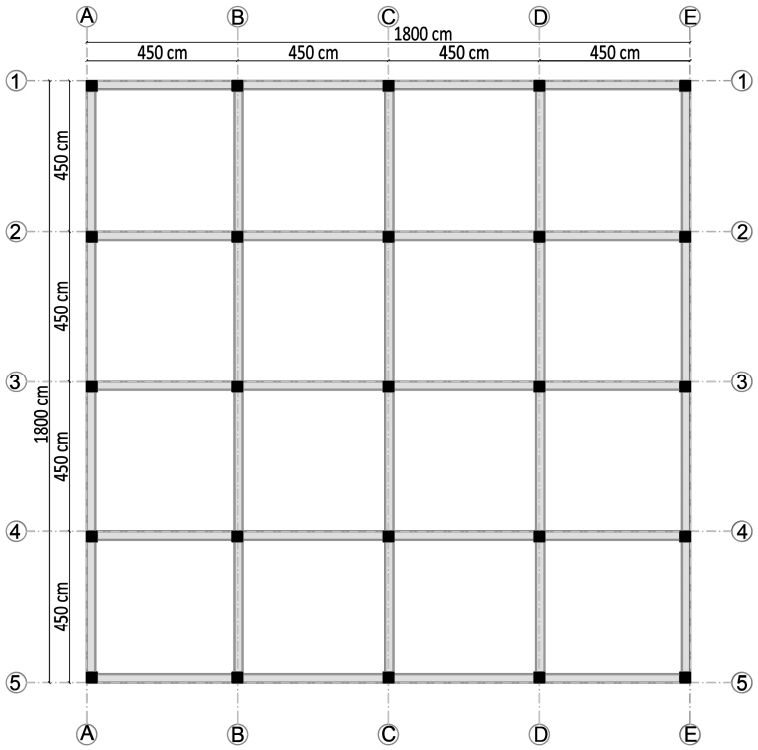

Figure 10. The blueprint of the selected RC structural model.

Pushover analysis, a numerical analysis method, examines how much structures or structural elements will deform under a certain load and how they will behave under the effect of these loads. In this type of analysis, elastic and plastic behaviors are generally taken into account. Pushover analysis is commonly used in earthquake engineering. This method is applied to predict how a structure will behave during an earthquake. Pushover analysis evaluates how much the structure will deform when pushed by static loads (usually with ground motion simulation) and at what point it may be damaged. It is simpler and can be completed more quickly than more complex dynamic analyses. This method allows for the assessment of displacement, rotation, and damage points of the structure [85–89]. The flow chart of the pushover analysis procedure is given in Figure 11.

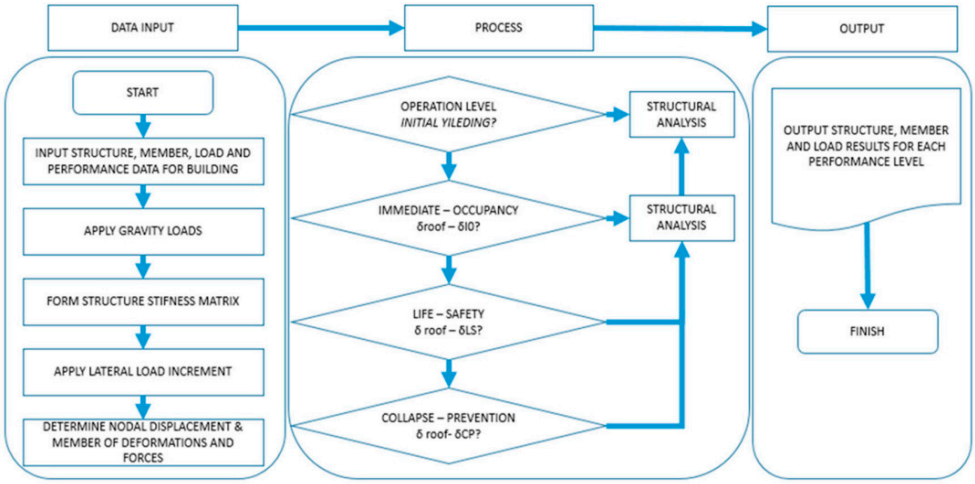

Figure 11. Flowchart of typical pushover analysis [90].

A target displacement value of 1.0 m was selected for all structural models. In the numerical analysis, the local soil class ZC soil class, which can be evaluated as the average soil class in Eurocode-8, was taken into account. Force-based plastic hinge frame elements (infrmFBPH) were chosen for the columns and beams in all structural models. These elements limit plasticity to a finite length and simulate force-based flexibility in extension. To accurately represent the stress-strain distribution within the section, an adequate number of fiber elements must be used. For the selected sections, a total of one hundred fiber elements were defined. The chosen plastic-hinge length (L_p/L) was set at 16.67%. The column boundary conditions were defined to match those of a cantilever, resulting in a fully fixed footing and a free top end. The structural properties of the RC building model are illustrated in Table 8.

Table 8. Structural properties of the RC structural model.

Parameters		Value
		Entire Structural Models
Concrete		25 MPa (C25)
Reinforcement		420 MPa (S420)
Beams (mm)		250 × 600
Height of floor (mm)		120
Story heights (mm)		3000
Concrete cover (mm)		25
Columns (mm)		400 × 400
Columns longitudinal reinforcement	Corners	4Φ20
	Top bottom	4Φ16
	Left Right	4Φ16
Columns transverse reinforcement		Φ8/150
Beam transverse reinforcement		Φ8/150
Used steel material		Pinto and Menegotto
Type of the constraint		Rigid diaphragm
Used concrete material		Mander
Local soil class		ZC
Incremental loads		5 kN
Permanent loads		5 kN/m
The damping ratio		5%
Importance class		II
Maximum displacement (m) (for 5-story)		1

The concrete grade was selected as C25/30 and the reinforcement material grade was selected as S420. Material grades for concrete and reinforcement are taken from the seismic design code in Türkiye. Modeling was done by taking into account the reinforcement and dimensional properties commonly used in mid-rise RC buildings.

When the performance limits of particular structural components are reached, it is critical to determine the target displacement for damage estimation in performance-based earthquake engineering. An internationally accepted method for estimating damage, structural analysis, took into account the limit states specified in Eurocode 8-Part 3 [91,92]. These states are categorized as damage limitation (DL), significant damage (SD), and near collapse (NC). The values for these limit states were calculated for each structural model. Table 9 provides thorough justifications for the limit state values that were considered during this study.

Table 9. Limit states in Eurocode [91,92].

Limit State	Description	Return Period (Year)	Probability of Exceedance (in 50 Years)
Damage limitation (DL)	Only lightly damaged; damage to non-structural components is economically repairable	225	0.20
Significant damage (SD)	Significantly damaged; some residual strength and stiffness; non-structural components damaged; uneconomic to repair	475	0.10
Near-collapse (NC)	Heavily damaged; very low residual strength and stiffness; large permanent drift but still standing	2475	0.02

The target displacements obtained using the measured and predicted PGA's within the scope of this study are shown on the typical pushover curve in Figure 12.

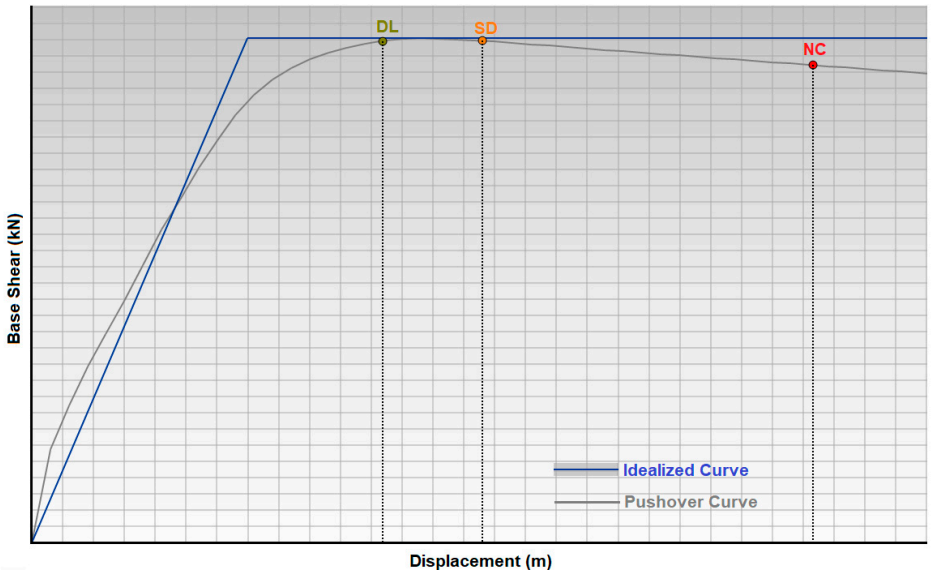

Figure 12. Typical pushover and idealized capacity curves.

In this study, target displacements (m) were first obtained separately for three different PGAs. Initially, target displacements were calculated using the highest measured PGAs from both earthquakes at the earthquake stations located in eleven provinces affected

by the 2023 Kahramanmaraş earthquakes. Subsequently, target displacements (m) for the predicted PGAs in the two earthquake codes and hazard maps used in Türkiye were obtained separately for the sample RC model. Structural analyses were carried out for the ground motion level, which had a 10% probability of being exceeded in 50 years (repetition period 475 years), a standard design earthquake ground motion level in the last two earthquake codes. Target displacements used to determine the performance of structures were obtained separately for the measured and predicted PGAs in the two most recent earthquake codes. The comparison of the target displacements for measured and predicted PGAs is illustrated in Table 10.

Table 10. Target displacements for the 2023 Kahramanmaraş earthquake region.

Province	Current Earthquake			TSDC-2007/DD-2			TBEC-2018/DD-2		
	DL (m)	SD (m)	NC (m)	DL (m)	SD (m)	NC (m)	DL (m)	SD (m)	NC (m)
Hatay	0.357	0.458	0.794	0.102	0.131	0.227	0.114	0.146	0.253
Kahramanmaraş	0.530	0.681	1.180	0.102	0.131	0.211	0.097	0.124	0.216
Adıyaman	0.229	0.294	0.509	0.077	0.098	0.170	0.061	0.079	0.137
Kilis	0.014	0.018	0.031	0.026	0.033	0.057	0.053	0.068	0.117
Diyarbakır	0.030	0.039	0.067	0.077	0.098	0.211	0.036	0.046	0.081
Şanlıurfa	0.062	0.080	0.138	0.051	0.065	0.113	0.028	0.036	0.062
Malatya	0.121	0.156	0.270	0.102	0.131	0.227	0.088	0.113	0.195
Osmaniye	0.087	0.112	0.195	0.102	0.131	0.227	0.079	0.102	0.176
Adana	0.105	0.134	0.233	0.077	0.098	0.170	0.059	0.076	0.132
Elazığ	0.018	0.023	0.040	0.077	0.098	0.170	0.102	0.131	0.227
Gaziantep	0.170	0.218	0.379	0.051	0.065	0.113	0.042	0.054	0.093

When Table 10 is examined, it is observed that the limit states are adequately represented for Kilis, Diyarbakır, and Elazığ provinces. However, the target displacement values predicted for the remaining provinces cannot adequately represent the target displacement values measured during earthquakes. For Hatay, Kahramanmaraş, Adıyaman, Şanlıurfa, Malatya, Osmaniye, Adana, and Gaziantep, where the target displacements were exceeded, the analyses were also performed for the recurrence period is 2475 years (ground motion level with a 2% probability of exceedance in 50 years). A comparison of the obtained limit state values is shown in Table 11.

Table 11. The comparison of target displacements for DD-1 with larger limit states for DD-2.

Province	Current Earthquake			TBEC-2018/DD-1		
	DL (m)	SD (m)	NC (m)	DL (m)	SD (m)	NC (m)
Hatay	0.357	0.458	0.794	0.228	0.291	0.505
Kahramanmaraş	0.530	0.681	1.180	0.178	0.229	0.397
Adıyaman	0.229	0.294	0.509	0.106	0.137	0.238
Şanlıurfa	0.062	0.080	0.138	0.056	0.072	0.125
Malatya	0.121	0.156	0.270	0.165	0.212	0.368
Osmaniye	0.087	0.112	0.195	0.154	0.198	0.343
Adana	0.105	0.134	0.233	0.115	0.147	0.255
Gaziantep	0.170	0.218	0.379	0.082	0.105	0.182

The obtained results also coincide with the damage distribution findings made after the earthquake. It is especially evident that the larger-than-expected acceleration values largely ignored ground conditions. Its importance in terms of revealing its effect has been emphasized once again. While the largest earthquake ground motion level, DD-1, was not exceeded for Osmaniye and Adana, it was exceeded for other provinces. This clearly

indicates that the earthquake hazards were larger than the predicted earthquake hazards for these provinces.

5. Results and Conclusions

With today's technology, it does not seem feasible to predict the time, size, and location of earthquakes. Earthquake hazards for any region can be estimated using different methods, and with these estimates, seismic parameters can be obtained for any region or geographical location. In this study, the seismic parameters of eleven provinces affected by the 6 February 2023, Kahramanmaraş earthquake, which caused great destruction in Türkiye, were analyzed. When PGA values were compared in the provinces affected by the February 6 earthquake, two different situations were encountered. In provinces such as Diyarbakır, Osmaniye, Kilis, Adana, and Elazig, which are further away from the earthquake center, the expected PGA values were met. However, PGA values were recorded much higher than expected in the provinces of focus, especially in Kahramanmaraş, Adıyaman, and Hatay. As it is known, PGA values are a parameter that directly changes with ground conditions. It was studied with the assumption that the V_{s30} values in the stations where the acceleration values measured while accelerating the earthquake hazard map of Türkiye were above 760 m/s. However, it is also seen in the published information of the stations that many stations are not qualified during the location selection of the registration stations. In this case, it was observed that the expected PGA values at nearby stations were exceeded by the effect of ground magnifications. This situation can also be evaluated positively for subsequent studies and may reveal how important ground enlargements are in the design phase and should be taken into account first. Specifically, the PGA and S_{DS} values for the geographical location were compared according to the last two earthquake hazard maps. It seems that PGA values measured during earthquakes exceed the values predicted in earthquake hazard maps in most provinces. Target displacements for a sample RC structure were obtained separately for each province, taking into account the largest PGA values predicted in the earthquake hazard maps and the values measured during earthquakes. It should be taken into consideration that damage scenarios and performance levels will not be very realistic in structures where the target displacement value is not met. In the provinces where the target displacement limit states for the standard design ground motion level are not met, new structural analyses were performed by considering the largest earthquake ground motion level. Despite this, there are still many provinces where target displacement limit values are not met. This reveals the necessity of conducting geographical location-specific seismic hazard analyses. Accurately representing the earthquake hazard ensures that the earthquake performance of buildings is more meaningful.

Statistical studies are limited to the selection of sampling intervals. Earthquake hazard maps made at the macro level are naturally created with very wide sampling intervals. Although the previous hazard maps used in Türkiye and the PGA values obtained from them are informative, they are not sufficient during the implementation phase. The reason for this is that the ground conditions are mostly based on assumptions. For this reason, soil classifications based on microzonation should be made first of all and the expected PGA value for each different soil environment should be defined separately. Otherwise, it will be inevitable that the expected PGA values will be exceeded.

The current earthquake hazard map used in Türkiye is obtained specifically for each geographical location. However, in the previous earthquake zone map, seismic hazard was assessed on a regional basis. It should be acknowledged that this is a significant achievement. Seismic parameters obtained specifically for each location have influenced the target displacements obtained. In addition, considering the large earthquakes that have occurred, it reveals the necessity of re-performing seismic hazard analyses, especially for the

provinces in the earthquake zone. The anticipated PGA, spectral acceleration coefficients, and the idealized curve for target displacements in TBEC-2018 should be revised based on the recent Kahramanmaraş earthquakes. Accurate representation of the PGA value allows the design spectra used in structural analyses to be more realistic and to obtain accurate damage estimates that may occur in earthquakes. The accelerations of the Kahramanmaraş earthquakes were high enough to cause large-scale destruction and shaking. This indicates that construction standards, ground analyses, and general earthquake preparations in the region need to be further improved.

In this paper, the damages commonly observed in the earthquake region were specifically examined for RC structures. Incomplete or non-existent use of earthquake-resistant building design principles in the planning and construction phase is one of the important causes of damage. It can be stated that the building inspection mechanisms implemented in Türkiye, especially in the last decade, have significantly reduced damage levels. In addition, poor workmanship and low material strength have also contributed to the damage rate. Factors such as soft or weak stories, inadequate lateral stiffness, short columns, strong beams-weak columns, plan irregularities, and errors in reinforcement detailing pertaining to the processing of reinforcement (insufficient stirrups, inadequate or missing rebar layouts, inadequate or incorrect interlocking), have negatively affected the performances of the buildings, thereby influencing the level of structural damage. At this point, applying the principles outlined in the regulation with adequate supervision during both the construction and project phases could be seen as the primary step in minimizing the troubles. Besides, irregularities like soft or weak stories and short columns that might negatively affect the behavior of buildings under the influence of earthquake loads, must be avoided as much as possible, or else, required protection must be taken.

It has been observed that a large portion of structures subject to partial or total collapse in earthquakes are made up of RC frames only. In structures where RC shear walls are used, damages have been quite limited, or life safety has been ensured. In this context, the use of RC shear walls, which are not mandatory in the ground and upper floors of RC structures in the earthquake regulations currently used in Türkiye, should be made mandatory. Thus, it is used to increase the rigidity of the structure in earthquake zones and to enable it to carry horizontal loads (such as earthquake effects) more efficiently.

In addition, RC structures constructed in adjacent arrangements should be avoided as much as possible, and if necessary, collision effects should be minimized by using expansion joints. In order to increase the building area, the use of heavy overhangs on upper floors should be restricted. In RC structures, the heights and purpose of use within the structure should not be changed. The building control mechanism used in Türkiye in recent years should continue to be applied more sensitively both in the project and construction phases. This process, which is applied to urban building stock, should also be used in rural areas. In addition to all these, with the help of structural health monitoring applications to be created for the structures, the traceability of the structures can be ensured, allowing the necessary interventions to be made before a possible earthquake.

Author Contributions: Conceptualization, E.I., A.B. and E.A.; methodology, E.I., F.A. and E.A.; validation, A.B. and E.I.; investigation, E.I., F.A. and A.B.; resources, F.A. and A.B.; data curation, A.B. and E.A.; writing—original draft preparation, E.I., A.B. and F.A.; writing—review and editing, E.A.; visualization, E.A.; supervision, E.I. and F.A.; funding acquisition, E.I., F.A., A.B. and E.A. All authors have read and agreed to the published version of the manuscript.

Funding: This research received no external funding.

Institutional Review Board Statement: Not applicable.

Informed Consent Statement: Not applicable.

Data Availability Statement: Data are contained within the article.

Conflicts of Interest: The authors declare no conflict of interest.

References

1. Goda, K.; Kiyota, T.; Pokhrel, R.M.; Chiaro, G.; Katagiri, T.; Sharma, K.; Wilkinson, S. The 2015 Gorkha Nepal earthquake: Insights from earthquake damage survey. *Front. Built Environ.* **2015**, *1*, 8.
2. Milani, G.; Valente, M. Failure analysis of seven masonry churches severely damaged during the 2012 Emilia-Romagna (Italy) earthquake: Non-linear dynamic analyses vs conventional static approaches. *Eng. Fail. Anal.* **2015**, *54*, 13–56.
3. Zhang, M.; Jin, Y. Building damage in Dujiangyan during the Wenchuan earthquake. *Earthq. Eng. Eng. Vib.* **2008**, *7*, 263–269.
4. Clifton, C.; Bruneau, M.; MacRae, G.; Leon, R.; Fussell, A. Steel structures damage from the Christchurch earthquake series of 2010 and 2011. *Bull. N. Z. Soc. Earthq. Eng.* **2011**, *44*, 297–318.
5. Lagomarsino, S. Damage assessment of churches after L'Aquila earthquake (2009). *Bull. Earthq. Eng.* **2012**, *10*, 73–92.
6. Mimura, N.; Yasuhara, K.; Kawagoe, S.; Yokoki, H.; Kazama, S. Damage from the Great East Japan Earthquake and Tsunami—A quick report. *Mitig. Adapt. Strateg. Glob. Change* **2011**, *16*, 803–818. [CrossRef]
7. Mangalathu, S.; Sun, H.; Nweke, C.C.; Yi, Z.; Burton, H.V. Classifying earthquake damage to buildings using machine learning. *Earthq. Spectra* **2020**, *36*, 183–208. [CrossRef]
8. Valente, M.; Milani, G. Earthquake-induced damage assessment and partial failure mechanisms of an Italian Medieval castle. *Eng. Fail. Anal.* **2019**, *99*, 292–309.
9. Stepinac, M.; Lourenço, P.B.; Atalić, J.; Kišiček, T.; Uroš, M.; Baniček, M.; Novak, M.Š. Damage classification of residential buildings in historical downtown after the ML5. 5 earthquake in Zagreb, Croatia in 2020. *Int. J. Risk Reduct.* **2021**, *56*, 102140.
10. Ademović, N.; Toholj, M.; Radonić, D.; Casarin, F.; Komesar, S.; Ugarković, K. Post-earthquake assessment and strengthening of a cultural-heritage residential masonry building after the 2020 Zagreb earthquake. *Buildings* **2022**, *12*, 2024. [CrossRef]
11. Pantò, B.; Grosman, S.; Macorini, L.; Izzuddin, B.A. A macro-modelling continuum approach with embedded discontinuities for the assessment of masonry arch bridges under earthquake loading. *Eng. Struct.* **2022**, *269*, 114722.
12. Naik, S.P.; Mohanty, A.; Mittal, H.; Porfido, S.; Michetti, A.M.; Yang, B.M.; Gwon, O.; Kim, Y.S. The earthquake environmental effects (EEEs) of the 6th February 2018, Hualien earthquake (Mw = 6.4): A contribution to the seismic hazard estimation in the epicentral area. *Quat. Int.* **2023**, *656*, 48–69.
13. Naik, S.P.; Reicherter, K.; Kázmér, M.; Skapski, J.; Mohanty, A.; Kim, Y.S. Archeoseismic study of damage in medieval monuments around New Delhi, India: An approach to understandingpaleoseismicity in an Intraplate Region. *GeoHazards* **2024**, *5*, 142–165.
14. Sugimori, R. Damage by the 1855 Edo earthquake and response to the disaster—Study based on Edo Ohjishin no Zu (Picture Scroll of the 1855 Edo Earthquake). *J. Disaster Res.* **2024**, *19*, 38–49. [CrossRef]
15. Qu, Z.; Zhu, B.; Cao, Y.; Fu, H. Rapid report of seismic damage to buildings in the 2022 M 6.8 Luding earthquake, China. *Earthq. Res. Adv.* **2023**, *3*, 100180.
16. Tena-Colunga, A. Conditions of structural irregularity. Relationships with observed earthquake damage in Mexico City in 2017. *Soil Dyn. Earthq. Eng.* **2021**, *143*, 106630.
17. Nemutlu, O.F.; Balun, B.; Sari, A. Damage assessment of buildings after 24 January 2020 Elazığ-Sivrice earthquake. *Earthq. Struct.* **2021**, *20*, 325–335.
18. Isik, E.; Aydin, M.C.; Buyuksarac, A. 24 January 2020 Sivrice (Elazığ) earthquake damages and determination of earthquake parameters in the region. *Earthq. Struct.* **2020**, *19*, 145–156.
19. Caglar, N.; Vural, I.; Kirtel, O.; Saribiyik, A.; Sumer, Y. Structural damages observed in buildings after the January 24, 2020 Elazığ-Sivrice earthquake in Türkiye. *Case Stud. Constr. Mater.* **2023**, *18*, e01886.
20. Işık, E. Structural failures of adobe buildings during the February 2023 Kahramanmaraş (Türkiye) earthquakes. *Appl. Sci.* **2023**, *13*, 8937. [CrossRef]
21. Avcil, F. Investigation of Precast Reinforced Concrete Structures during the 6 February 2023 Türkiye Earthquakes. *Sustainability* **2023**, *15*, 14846. [CrossRef]
22. İnce, O. Structural damage assessment of reinforced concrete buildings in Adıyaman after Kahramanmaraş (Türkiye) Earthquakes on 6 February 2023. *Eng. Fail. Anal.* **2024**, *156*, 107799. [CrossRef]
23. Ivanov, M.L.; Chow, W.K. Structural damage observed in reinforced concrete buildings in Adiyaman during the 2023 Turkiye Kahramanmaras Earthquakes. *Structures* **2023**, *58*, 105578. [CrossRef]
24. Işık, E.; Avcil, F.; İzol, R.; Büyüksaraç, A.; Bilgin, H.; Harirchian, E.; Arkan, E. Field reconnaissance and earthquake vulnerability of the rc buildings in Adıyaman during 2023 Türkiye Earthquakes. *Appl. Sci.* **2024**, *14*, 2860. [CrossRef]
25. Yuzbasi, J. Post-Earthquake Damage Assessment: Field Observations And Recent developments with recommendations from the Kahramanmaraş earthquakes in Türkiye on February 6th, 2023 (Pazarcık M7.8 and Elbistan M7.6). *J. Earthq. Eng.* **2024**, 1–26. [CrossRef]

26. Cetin, K.O.; Cuceoglu, F.; Ayhan, B.U.; Yildirim, S.; Aydin, S.; Demirdogen, S.; Er, Y.; Gurbuz, A.; Moss, R.E.S. Performance of hydraulic structures during 6 February 2023 Kahramanmaraş, Türkiye, earthquake sequence. *Earthq. Spectra* **2024**, *40*, 2231–2267. [CrossRef]
27. Bol, E.; Özocak, A.; Sert, S.; Çetin, K.Ö.; Arslan, E.; Kocaman, K.; Ayhan, B.U. Evaluation of soil liquefaction in the city of Hatay triggered after the February 6, 2023 Kahramanmaraş-Türkiye earthquake sequence. *Eng. Geol.* **2024**, *339*, 107648. [CrossRef]
28. Arslan, M.H.; Dere, Y.; Ecemiş, A.S.; Doğan, G.; Özturk, M.; Korkmaz, S.Z. Code-based damage assessment of existing precast industrial buildings following the February 6th, 2023 Kahramanmaraş earthquakes (Pazarcık Mw 7.7 and Elbistan Mw7.6). *J. Build. Eng.* **2024**, *86*, 108811. [CrossRef]
29. Avğın, S.; Köse, M.M.; Özbek, A. Damage assessment of structural and geotechnical damages in Kahramanmaraş during the February 6, 2023 earthquakes. *Eng. Sci. Technol. Int. J.* **2024**, *57*, 101811. [CrossRef]
30. Binici, B.; Yakut, A.; Kadas, K.; Demirel, O.; Akpinar, U.; Canbolat, A.; Yurtseven, F.; Oztaskin, O.; Aktas, S.; Canbay, E. Performance of RC buildings after Kahramanmaraş Earthquakes: Lessons toward performance based design. *Earthq. Eng. Eng. Vibr.* **2023**, *22*, 883–894. [CrossRef]
31. Demir, A.; Celebi, E.; Ozturk, H.; Ozcan, Z.; Ozocak, A.; Bol, E.; Sert, S.; Sahin, F.Z.; Arslan, E.; Dere Yaman, Z.; et al. Destructive impact of successive high magnitude earthquakes occurred in Türkiye's Kahramanmaraş on February 6, 2023. *Bull. Earthq. Eng.* **2024**, *23*, 893–919. [CrossRef]
32. Ozturk, M.; Arslan, M.H.; Korkmaz, H.H. Effect on RC buildings of 6 February 2023 Turkey earthquake doublets and new doctrines for seismic design. *Eng. Fail. Anal.* **2024**, *153*, 107521. [CrossRef]
33. Nemutlu, Ö.F.; Sarı, A.; Balun, B. 06 Şubat 2023 Kahramanmaraş depremlerinde (Mw 7.7–Mw 7.6) meydana gelen gerçek can kayıpları ve yapısal hasar değerlerinin tahmin edilen değerler ile karşılaştırılması. *Afyon Kocatepe Üniversitesi Fen Ve Mühendislik Bilim. Derg.* **2023**, *23*, 1222–1234. [CrossRef]
34. Balun, B. Assessment of seismic parameters for 6 February 2023 Kahramanmaraş earthquakes. *Struct. Eng. Mech.* **2023**, *88*, 117.
35. Sivrikaya, O.; Türker, E.; Cüre, E.; Atmaca, E.E.; Angin, Z.; Başağa, H.B.; Altunişik, A.C. Impact of soil conditions and seismic codes on collapsed structures during the 2023 Kahramanmaraş earthquakes: An in-depth study of 400 reinforced concrete buildings. *Soil Dyn. Earthq. Eng.* **2025**, *190*, 109119. [CrossRef]
36. Altunişik, A.C.; Arslan, M.E.; Kahya, V.; Aslan, B.; Sezdirmez, T.; Dok, G.; Kirtel, O.; Öztürk, H.; Sunca, F.; Baltaci, A.; et al. Field observations and damage evaluation in reinforced concrete buildings after the February 6th, 2023, Kahramanmaraş–Türkiye Earthquakes. *J. Earthq. Tsun.* **2023**, *17*, 2350024. [CrossRef]
37. Şen, F.; Sunca, F.; Altunişik, A.C. Seismic performance assessment of a base-isolated hospital building subjected to February 6, 2023, Kahramanmaraş, Türkiye earthquakes (Mw 7.7 Pazarcık and Mw 7.6 Elbistan) and seismic fragility analysis considering different construction stages. *Soil Dyn. Earthq. Eng.* **2024**, *185*, 108876. [CrossRef]
38. Erbaş, Y.; Mercimek, Ö.; Anıl, Ö.; Çelik, A.; Akkaya, S.T.; Kocaman, İ.; Gürbüz, M. Design deficiencies, failure modes and recommendations for strengthening in reinforced concrete structures exposed to the February 6, 2023 Kahramanmaraş Earthquakes (Mw 7.7 and Mw 7.6). *Nat. Hazards* **2024**, *121*, 3153–3194. [CrossRef]
39. Akar, F.; Işık, E.; Avcil, F.; Büyüksaraç, A.; Arkan, E.; İzol, R. Geotechnical and structural damages caused by the 2023 Kahramanmaraş Earthquakes in Gölbaşı (Adıyaman). *Appl. Sci.* **2024**, *14*, 2165. [CrossRef]
40. Flora, A.; Bilotta, E.; Valtucci, F.; Fierro, T.; Perez, R.; de Magistris, F.S.; Modoni, G.; Spacagna, R.; Kelesoglu, M.K.; Sargin, S.; et al. Liquefaction effects in the city of Gölbaşı: From the analysis of predisposing factors to damage survey. *Eng. Geol.* **2024**, *338*, 107633. [CrossRef]
41. Tapia-Hernández, E.; Geneş, M.C.; Gülkan, P. Damage assessment and seismic response of steel buildings during the Kahramanmaraş, Turkey earthquakes of February 6, 2023. *Earthq. Spectra* **2024**. [CrossRef]
42. Tapia-Hernández, E.; Geneş, M.C.; Guerrero-Bobadilla, H. Structural behavior of hospitals during the Kahramanmaraş earthquake of February 6, 2023. *Earthq. Spectra* **2024**, 87552930241298678.
43. Tan, M.; Avşar, Ö.; Yıldızhan, F.; Atmaca, N. Effect of infill walls on the seismic performance of a severely damaged substandard RC building during the February 6, 2023, Kahramanmaras earthquake sequence. *Eng. Fail. Anal.* **2025**, *169*, 109117.
44. Işık, E.; Hadzima-Nyarko, M.; Avcil, F.; Büyüksaraç, A.; Arkan, E.; Alkan, H.; Harirchian, E. Comparison of seismic and structural parameters of settlements in the East Anatolian Fault Zone in light of the 6 February Kahramanmaraş earthquakes. *Infrastructures* **2024**, *9*, 219. [CrossRef]
45. Yön, B.; Dedeoğlu, İ.Ö.; Yetkin, M.; Erkek, H.; Calayır, Y. Evaluation of the seismic response of reinforced concrete buildings in the light of lessons learned from the February 6, 2023, Kahramanmaraş, Türkiye earthquake sequences. *Nat. Hazards* **2024**, *121*, 873–909.
46. Mertol, H.C.; Tunç, G.; Akış, T.; Kantekin, Y.; Aydın, İ.C. Investigation of RC buildings after 6 February 2023, Kahramanmaraş, Türkiye earthquakes. *Buildings* **2023**, *13*, 1789. [CrossRef]
47. Vuran, E.; Serhatoğlu, C.; Timurağaoğlu, M.Ö.; Smyrou, E.; Bal, İ.E.; Livaoğlu, R. Damage observations of RC buildings from 2023 Kahramanmaraş earthquake sequence and discussion on the seismic code regulations. *Bull. Earthq. Eng.* **2024**, *23*, 1153–1182.

48. Ozdemir, A. Examining the effect of structural characteristics of Antakya building stock on the damage level after the Kahramanmaraş earthquakes. *J. Earthq. Eng.* **2024**, 1–30. [CrossRef]
49. Sezgin, S.K.; Sakcalı, G.B.; Özen, S.; Yıldırım, E.; Avcı, E.; Bayhan, B.; Çağlar, N. Reconnaissance report on damage caused by the February 6, 2023, Kahramanmaraş Earthquakes in reinforced-concrete structures. *J. Build. Eng.* **2024**, *89*, 109200. [CrossRef]
50. Doğruyol, M. Characterisation of acrylic copolymer treated concretes and concretes of reinforced concrete buildings collapsed in the 6 February 2023 Mw = 7.8 Kahramanmaraş (Türkiye) earthquake. *Eng. Fail. Anal.* **2024**, *161*, 108249. [CrossRef]
51. Ulutaş, H. Investigation of the causes of soft-storey and weak-storey formations in low-and mid-rise rc buildings in Türkiye. *Buildings* **2024**, *14*, 1308. [CrossRef]
52. Apostolaki, S.; Riga, E.; Pitilakis, D. Rapid damage assessment effectiveness for the 2023 Kahramanmaraş Türkiye earthquake sequence. *Int. J. Dis. Risk Reduct.* **2024**, *111*, 104691.
53. Özman, G.Ö.; Selçuk, S.A.; Arslan, A. Image classification on post-earthquake damage assessment: A case of the 2023 Kahramanmaraş earthquake. *Eng. Sci. Technol. Int. J.* **2024**, *56*, 101780.
54. Gencturk, B.; Sezen, H.; Mieler, M.; Griffith, M.; Gudhka, P.; Garai, R. Vulnerability assessment of buildings in the aftermath of 2023 Turkiye earthquake sequence. *Earthq. Spectra* **2025**, 87552930241307884.
55. Işık, E.; Kutanis, M. Determination of local site-specific spectra using probabilistic seismic hazard analysis for Bitlis Province, Turkey. *Earth Sci. Res. J.* **2015**, *19*, 129–134.
56. Arslan, M.H.; Köroğlu, M.A.; Köken, A. Binaların yapısal performansının statik itme analizi ile belirlenmesi. *Yapı Teknol. Elektron. Derg.* **2008**, *4*, 71–84.
57. Tekin, M.; Erdem, R.T.; Gündüz, C. Betonarme bir yapının performansa dayalı tasarımı: Deplasmana dayalı sismik yaklasım ve yerdeğistirme katsayıları yöntemi-performance–based desıgn of a reınforced concrete structure: Dısplacement–based seısmıc approach and dısplacement coeffıcıents. *Celal Bayar Univ. J. Sci.* **2011**, *7*, 1–11.
58. Becker, R. Fundamentals of performance-based building design. In *Building Simulation*; Springer: Berlin/Heidelberg, Germany, 2008; Volume 1, pp. 356–371.
59. Aydınoğlu, M.N. A response spectrumbased nonlinear assessment tool for practice: Incremental response spectrum analysis (IRSA). *ISET J. Earthq. Technol.* **2007**, *44*, 169–192.
60. Doran, B.; Akbaş, B.; Sayım, İ.; Fahjan, Y.; Alacalı, S.N. Uzun periyotlu bir yapıda yapısal sağlık izlemesi ve deprem performansının belirlenmesi. In Proceedings of the Turkey Conference on Earthquake Engineering and Seismology, Ankara, Türkiye, 11–14 October 2011.
61. Kutanis, M.; Boru, O.E. The need for upgrading the seismic performance objectives. *Earthq. Struct.* **2014**, *7*, 401–414.
62. Güneş, N.; Ulucan, Z.Ç.; Erdoğan, A.S. Yakın fay yer hareketlerinin yön etkisi. *Niğde Ömer Halisdemir Üniversitesi Mühendislik Bilim. Derg.* **2013**, *2*, 21–33.
63. Güneş, N. Yakın Fay yer Hareketleri ve Performansa Dayalı Tasarıma Uyarlanmaları. Ph.D. Thesis, Fırat Üniversitesi, Fen Bilimleri Enstitüsü, Elâzığ, Türkiye, 2009.
64. Isik, E. A comparative analysis of seismic and structural parameters for historical period earthquakes in Türkiye. *Earthq. Struct.* **2023**, *24*, 377–391.
65. Isık, E. Comparative investigation of seismic and structural parameters of earthquakes (M $\geq$ 6) after 1900 in Turkey. *Arab. J. Geosci.* **2022**, *15*, 971. [CrossRef]
66. Maidi, M.; Shufrin, I. Evaluation of existing reinforced concrete buildings for seismic retrofit through external stiffening: Limit displacement method. *Buildings* **2024**, *14*, 2781. [CrossRef]
67. Bilgin, H.; Hadzima-Nyarko, M.; Işık, E.; Ozmen, H.B.; Harirchian, E. A comparative study on the seismic provisions of different codes for RC buildings. *Struct. Eng. Mech.* **2022**, *83*, 195–206.
68. Ricci, P.; Di Domenico, M.; Verderame, G.M. Effects of the in-plane/out-of-plane interaction in URM infills on the seismic performance of RC buildings designed to Eurocodes. *J. Earthq. Eng.* **2022**, *26*, 1595–1629.
69. Khan, R.A. Performance based seismic design of reinforced concrete building. *Int. J. Innov. Res. Sci. Eng. Technol.* **2014**, *3*, 13495–13506.
70. Emre, Ö.; Duman, T.Y.; Özalp, S.; Şaroğlu, F.; Olgun, Ş.; Elmacı, H.; Çan, T. Active fault database of Turkey. *Bull. Earthq. Eng.* **2018**, *16*, 3229–3275.
71. Alkan, H.; Büyüksaraç, A.; Bektaş, Ö.; Işık, E. Coulomb stress change before and after 24.01. 2020 Sivrice (Elazığ) earthquake (Mw = 6.8) on the East Anatolian Fault Zone. *Arab. J. Geosci.* **2021**, *14*, 2648.
72. Ergin, K. A catalogue of earthquakes for Turkey and surrounding area (11AD to 1964AD). *Tech. Univ. Mining Eng. Fac. Publ.* **1967**, *24*, 189.
73. Willis, B. World Earthquake Belts. *Sci. Am.* **1928**, *138*, 306–309. [CrossRef]
74. Sieberg, A. *Untersuchungen über Erdbeben und Bruchschollenbau im Östlichen Mittelmeergebiet*; Gustav Fischer: Jena, Germany, 1932.
75. Ambraseys, N.N. Some characteristic features of the Anatolian fault zone. *Tectonophysics* **1970**, *9*, 143–165.

76. Soysal, H.; Sipahioğlu, S.; Kolçak, D.; Altınok, Y. *Historical Earthquake Catalogue of Turkey and Surrounding Area (2100 BC–1900 AD)*; Technical Report, TÜBİTAK, No. TBAG-341; The Scientific and Technological Research Council of Turkey: Ankara, Türkiye, 1981.
77. Işık, E.; Ekinci, Y.L.; Sayıl, N.L.; Büyüksaraç, A.; Aydin, M.C. Time-dependent model for earthquake occurrence and effects of design spectra onstructural performance: A case study from the North Anatolian Fault Zone, Turkey. *Turk. J. Earth Sci.* **2021**, *30*, 215–234.
78. AFAD-TADAS. Disaster and Emergency Management Presidency Department of Earthquake Turkish Accelerometric Database and Analysis System. 2023. Available online: https://tadas.afad.gov.tr/ (accessed on 15 June 2024).
79. AFAD. 2024. Available online: https://tdth.afad.gov.tr (accessed on 15 October 2024).
80. TBEC. *Turkish Building Earthquake Code*; T.C. Resmi Gazete: Ankara, Türkiye, 2018.
81. Yao, C.; Zhong, H.; Zhu, Z. Development of a large shaking table test for sand liquefaction analysis. *Lithosphere* **2024**, *2*, 137.
82. Zhu, Z.; Zhang, F.; Peng, Q.; Dupla, J.C.; Canou, J.; Cumunel, G.; Foerster, E. Effect of the loading frequency on the sand liquefaction behaviour in cyclic triaxial tests. *Soil Dyn. Earthq. Eng.* **2021**, *147*, 106779.
83. Cetin, K.O.; Cakir, E.; Eyigün, Y.; Gokceoglu, C. Soil liquefaction manifestations at Hatay Airport after the February 2023 Türkiye earthquake sequence. *Earthq. Spectra* **2025**, *41*, 290–321.
84. Seismosoft. SeismoStruct 2024—A Computer Program for Static and Dynamic Nonlinear Analysis of Framed Structures. 2024. Available online: http://www.seismosoft.com (accessed on 10 February 2024).
85. Chopra, A.K.; Goel, R.K. A modal pushover analysis procedure for estimating seismic demands for buildings. *Earthq. Eng. Struct. Dyn.* **2002**, *31*, 561–582.
86. Antoniou, S.; Pinho, R. *Seismostruct–Seismic Analysis Program by Seismosoft*; Technical Manual and User Manual; Seismosoft: Pavia, Italy, 2022.
87. Krawinkler, H.; Seneviratna, G.D.P.K. Pros and cons of a pushover analysis of seismic performance evaluation. *Eng. Struct.* **1998**, *20*, 452–464.
88. Elnashai, A.S. Advanced inelastic static (pushover) analysis for earthquake applications. *Struct. Eng. Mech.* **2001**, *12*, 51–69.
89. Borzi, B.; Pinho, R.; Crowley, H. Simplified pushover-based vulnerability analysis for large-scale assessment of RC buildings. *Eng. Struct.* **2008**, *30*, 804–820.
90. Işık, M.F.; Avcil, F.; Harirchian, E.; Bülbül, M.A.; Hadzima-Nyarko, M.; Işık, E.; İzol, R.; Radu, D. A Hybrid Artificial Neural Network—Particle Swarm Optimization Algorithm Model for the Determination of Target Displacements in Mid-Rise Regular Reinforced-Concrete Buildings. *Sustainability* **2023**, *15*, 9715. [CrossRef]
91. *EN 1998-3*; Eurocode-8: Design of Structures for Earthquake Resistance-Part 3: Assessment and Retrofitting of Buildings. European Committee for Standardization: Bruxelles, Belgium, 2005.
92. Pinto, P.E.; Franchin, P. Eurocode 8-Part 3: Assessment and retrofitting of buildings. In Proceedings of the Eurocode 8 Background and Applications, Dissemination of Information for Training, Lisbon, Portugal, 10–11 February 2011.